ACS APPLIED MATERIALS & INTERFACES

Research Article

www.acsami.org

# Ternary Ag/Epoxy Adhesive with Excellent Overall Performance

Yan-Hong Ji,[†,‡] Yu Liu,[†] Gui-Wen Huang,[†] Xiao-Jun Shen,[§] Hong-Mei Xiao,[†] and Shao-Yun Fu*[,†]

[†]Technical Institute of Physics and Chemistry, Chinese Academy of Sciences, Beijing 100190, China

[‡]University of Chinese Academy of Sciences, Beijing 100049, China

[§]Materials and Textile Engineering College, Jiaxing University, Jiaxing 314001, Zhejiang Province China

Supporting Information

**ABSTRACT:** Excellent electrical conductivity (EC) generally conflicts with high lap shear strength (LSS) for electrically conductive adhesives (ECAs) since EC increases while LSS decreases with increasing conductive filler content. In this work, the ECAs with the excellent overall performance are developed based on the ternary hybrid of Ag microflakes (Ag-MFs), Ag nanospheres (Ag-NSs), and Ag nanowires (Ag-NWs). First, a low silver content adhesive system is determined. Then, the effects of the relative contents of Ag fillers on the EC and the LSS are studied. It is shown that a small amount of Ag-NSs or Ag-NWs can dramatically improve the EC for the Ag-MF/epoxy adhesives. The Ag-NSs and Ag-NWs with appropriate contents have a synergistic effect in improving the EC. Meanwhile, the LSS of the as-prepared adhesive with the appropriate Ag contents reaches an optimal value. Both the EC and the LSS of the as-prepared ternary hybrid ECA with a low content of 40 wt % Ag are higher than those of the commercial ECAs filled with the Ag-MF content over 60 wt %. Finally, the ternary hybrid ECA with the optimal formulation is shown to be promising for printing the radio frequency identification tag antennas as an immediate application example.

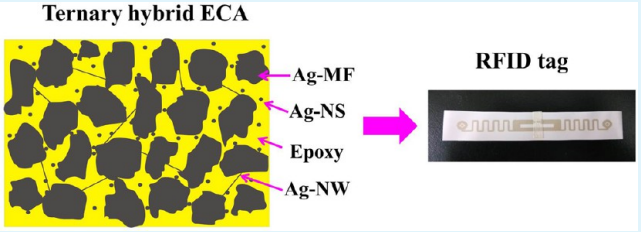


**KEYWORDS:** *electrically conductive adhesive, Ag microflake, Ag nanosphere, Ag nanowire, ternary hybrid*

## INTRODUCTION

As potentially excellent alternatives to solder, electrically conductive adhesives (ECAs) have been widely used in flip chip, printed circuit board, chip scale package, ball grid array, and three-dimensional stacking because of their environmental friendliness, mild processing conditions, low stress on substrates, and fine pitch interconnecting capability.[1−5] A typical ECA is made up of a polymeric matrix and conductive fillers. The polymeric matrix provides the mechanical properties while the conductive fillers contribute to the electrical conductivity (EC).[1,2,6,7] Epoxy resin is the most widely applied polymer matrix in the ECAs because of its low shrinkage, excellent adhesion, resistance to thermal and mechanical shocks, and outstanding resistance to moisture, solvents and chemical attacks.[8] Silver (Ag) is the most used conductive filler in the ECAs because of its stable chemical property and excellent conductive performance. In addition, the oxidation process of Ag in the air is extremely slow, and even its oxides are still conductive.[7,9]

The Ag fillers in the ECAs can be in the form of spheres, flakes, nanowires, and so on. Ag nanospheres (Ag-NSs) have been employed by Wu et al.[10] to synthesize the ECAs and it was found that the percolation threshold of the ECAs reached the lowest value when the average diameter of Ag-NSs was 50 nm. Ye et al.[11] reported that the ECA filled with Ag-NSs at the content of 70 wt % was not conductive while the ECAs filled with the same amount of Ag microspheres (Ag-MSs) had a good conductive ability. Among the Ag fillers, Ag microflakes (Ag-MFs) are the most commonly used conductive filler for commercial ECAs because of their high conductivity and relatively stable contact resistance. Therefore, much research has been conducted based on Ag-MFs,[12−15] and the EC of the ECAs filled with Ag-MFs was higher than that filled with Ag-NSs or Ag-MSs.[11,16] Recently, one-dimensional Ag nanowires (Ag-NWs) have attracted increasing interests due to their unique electrical, optical, and thermal properties and their potential applications in microelectronic, optoelectronic devices, and sensors.[17−20] Ag-NWs possess relatively higher aspect ratio compared to Ag-NSs or Ag-MFs, which may form ideal thermally or electrically conductive paths at a relatively lower percolation threshold in polymer adhesives.[7,21−23] To lower the costs, the ECAs have also been made from metal-coated fillers, such as Ag-coated carbon nanotubes,[24] Ag-coated graphite nanosheet,[9] Ag-coated polymer spheres,[25,26] Ag-coated basalt particles and basalt fibers,[27] and Ag-coated Cu particles and Cu flakes.[28,29] However, the ECAs containing metal-coated fillers usually have a relatively lower EC compared to those containing pure metal fillers.[27,28]

In general, it is not possible for a normal ECA made from single fillers to simultaneously possess both a high conductive performance and an excellent adhesive strength since these two properties generally conflict with each other. It is usually

Received: January 16, 2015
Accepted: April 2, 2015
Published: April 2, 2015





DOI: 10.1021/acsami.5b00470
ACS Appl. Mater. Interfaces 2015, 7, 8041−8052

needed to increase the content of conductive fillers to improve the EC of the ECAs. As a result, the content of Ag fillers of the ECAs in previous studies is in the range of ~60−94 wt %.[10−15] However, a high filler content will lead to a low adhesive property instead. Moreover, a higher content of conductive Ag fillers mean a higher cost for adhesives. So, it is not sensible to obtain high EC ECAs by simply increasing the content of conductive fillers. Therefore, some researchers turned to prepare the ECAs filled with the hybrid of two conductive fillers with different shapes and sizes.[30−39] The addition of Ag-NSs to the ECAs filled with Ag-MFs, or substitution of a part of Ag-MFs with Ag-NSs could obviously improve the EC of the ECAs.[30−37] Besides, the EC of the ECA filled with the binary hybrid of Ag-MFs and Ag nanodendrites is higher than that of the ECA filled with single Ag-MFs.[38] Moreover, the ECA filled with the binary hybrid of Ag-MFs and Ag nanobelts have a better conductive property than that filled with single Ag-MFs.[39] As mentioned above, Ag-NWs have a high aspect ratio, which is beneficial to formation of conductive pathways. However, the introduction of Ag-NWs (binary hybrid) or particularly both Ag-NWs and Ag-NSs (ternary hybrid) to Ag-MF ECAs have not been reported yet. It is expected that the addition of Ag-NWs or both Ag-NWs and Ag-NSs to the ECAs of Ag-MFs could bring about a great improvement in the EC. In addition, a higher LSS might be obtained if the total content of Ag fillers can be kept at a low level.

In this paper, the ECAs filled with Ag-MFs, Ag-NSs and Ag-NWs are prepared to develop ternary Ag/epoxy adhesives with an excellent overall performance. It is shown that a small amount of Ag-NSs or Ag-NWs can dramatically improve the EC of the ECAs filled with single Ag-MFs. And Ag-NWs can improve the EC to a much higher degree than Ag-NSs. Ag-NSs and Ag-NWs at appropriate contents in the ternary hybrid ECA have a synergistic effect in improving the EC. Moreover, a high lap shear strength (LSS) is also obtained for the as-prepared ternary hybrid ECA with an optimal formulation. Due to its excellent EC and high LSS, the obtained ternary Ag/epoxy adhesive with a low Ag content of 40 wt % is obviously superior to the traditional ECAs and the commercial adhesives with a much higher Ag-MF content over 60 wt %. Finally, the ternary hybrid ECA with the optimal formulation is successfully employed in printing the radio frequency identification (RFID) tag antenna as an immediate application example.

## EXPERIMENTAL SECTION

**Materials.** Silver nitrate ($AgNO_3$), hexahydrated ferric chloride ($FeCl_3·6H_2O$), ethylene glycol (EG), and poly(*N*-vinylpyrrolidone) (PVP, $M_w$ = ~85 000) were all purchased from Lan Yi Co. Ltd., Beijing, China. Epoxy was 4,5-epoxyclyclohexyl-1,2-diglycidyl diformate (TDE-85) obtained from Hunan Tuo Suo Technology Co. Ltd., China. It was a kind of trifunctional epoxy, and could exhibit high cure shrinkage when cured. It was reported that an ECA with a high cure shrinkage generally showed a high EC.[40] Curing agent was methylhexahydrophthalic anhydride (MeHHPA) purchased from Shanghai Li Yi Technology Development Co. Ltd., China. Catalyst was 2-ethyl-4-methylimidazole (2E4MZ) supplied by Changzhou Zhong Kai Chemical Co. Ltd., China. Coupling agent was γ-(2, 3-epoxypropoxy) propytrimethoxysilane (KH560) obtained from Shanghai Yao Hua Chemical Plant, China. Ag-MFs (SF-0340) were supplied by Kunming Noble Metal Electronic Materials Co. Ltd., China and Ag-NSs (S11000-25) were purchased from Ferro Corporation, USA. The particle size distributions of Ag-MFs and Ag-NSs are given in Supporting Information Table S1, and the morphologies of Ag-MFs and Ag-NSs are shown in Supporting Information Figure S1a and b, respectively. Two typical commercial ECAs were ABLEBOND84−1LMISR4 and CAPITON-924 K, which were purchased from Henkel AG & Co. KGaA, Germany and Shenzhen Capiton Sci-Technology Co. Ltd., China, respectively.

**Preparation of Ag-NWs.** Ag-NWs were synthesized via a hydrothermal synthetic method similar to that reported previously.[41−43] First, 200 mL EG solution of $FeCl_3·6H_2O$ (5.4 mg) was vigorously stirred after the addition of 3.33 g PVP. In the same time, 200 mL EG solution of $AgNO_3$ (3.4 g) was magnetically stirred. The two solutions were mixed drop by drop. Afterward, the obtained solution was transferred into an autoclave and heated at 160 °C for 2 h. After it was cooled to room temperature naturally, the solution was washed with a large amount of acetone and then with ethanol to separate Ag-NWs from EG. At last, Ag-NWs were dispersed in ethanol for further use.

**Preparation of ECAs.** First, epoxy (TDE-85), curing agent (MeHHPA), catalyst (2E4MZ), and coupling agent (KH560) were mixed uniformly. Second, the Ag-NW ethanol solution was added to the epoxy resin matrix. Then, the mixture obtained was put into a vacuum chamber (about 20 Pa) for 24 h to remove the solvent. Afterward, Ag-MFs (SF-0340) and Ag-NSs (S11000-25) were blended with the above mixture to prepare the ECAs according to the prescribed formulations of ECAs in Tables 1 and 2.

**Table 1. Formulation of ECAs Filled with Single Ag-MFs**

| Sample code | Epoxy resin (wt %) | Ag-MFs (wt %) | EC (Ω cm) |
|---|---|---|---|
| $F_{0.0}$ | 100 | 0.0 | $(2.03 \pm 0.11) \times 10^{14}$ |
| $F_{20.0}$ | 80 | 20.0 | $(5.40 \pm 0.12) \times 10^{1}$ |
| $F_{40.0}$ | 60 | 40.0 | $(3.78 \pm 0.07) \times 10^{-4}$ |
| $F_{60.0}$ | 40 | 60.0 | $(1.79 \pm 0.05) \times 10^{-4}$ |

**Table 2. Formulation of Binary and Ternary Hybrid ECAs with a 40 wt % Ag Content**

| Sample code | Epoxy resin (wt %) | Ag-MFs (wt %) | Ag-NSs (wt %) | Ag-NWs (wt %) |
|---|---|---|---|---|
| $F_{37.5}$ $S_{2.5}$ | 60 | 37.5 | 2.5 | 0 |
| $F_{35.0}$ $S_{5.0}$ | 60 | 35.0 | 5.0 | 0 |
| $F_{32.5}$ $S_{7.5}$ | 60 | 32.5 | 7.5 | 0 |
| $F_{30.0}$ $S_{10.0}$ | 60 | 30.0 | 10.0 | 0 |
| $F_{37.5}$ $W_{2.5}$ | 60 | 37.5 | 0 | 2.5 |
| $F_{35.0}$ $W_{5.0}$ | 60 | 35.0 | 0 | 5.0 |
| $F_{32.5}$ $W_{7.5}$ | 60 | 32.5 | 0 | 7.5 |
| $F_{30.0}$ $W_{10.0}$ | 60 | 30.0 | 0 | 10.0 |
| $F_{27.5}$ $W_{12.5}$ | 60 | 27.5 | 0 | 12.5 |
| $F_{25.0}$ $W_{15.0}$ | 60 | 25.0 | 0 | 15.0 |
| $F_{30.0}$ $S_{7.5}$ $W_{2.5}$ | 60 | 30.0 | 7.5 | 2.5 |
| $F_{30.0}$ $S_{5.0}$ $W_{5.0}$ | 60 | 30.0 | 5.0 | 5.0 |
| $F_{30.0}$ $S_{2.5}$ $W_{7.5}$ | 60 | 30.0 | 2.5 | 7.5 |

**Characterization and Measurements.** The morphologies of the Ag fillers and the ECAs were observed using a scanning electron microscope (SEM, Hitachi S-4300, Japan). The phase purity of Ag-NWs was characterized by X-ray diffraction (XRD) on an X-ray diffractometer with $CuK_\alpha$ radiation ($\lambda$ = 0.154 nm) between $2\theta = 10°$ and $2\theta = 90°$.

The samples for volume resistivity measurement were prepared according to the recommendation of GJB548A-1996. First, two parallel strips of 3 M tape were placed 2.54 mm apart along the length of a standard glass slide of 25.4 mm × 76.2 mm. Second, a small amount of the ECA was added in the space between the 3 M tapes. Then, a scalpel held manually at approximately 30° was used to squeeze the ECA into the 2.54 mm space. After the samples were heated at 150 °C for 2 h, the 3 M tapes were removed. The schematic of preparing the samples for EC measurement is presented in Supporting Information Figure S2a. The volume resistance of the


DOI: 10.1021/acsami.5b00470
ACS Appl. Mater. Interfaces 2015, 7, 8041−8052

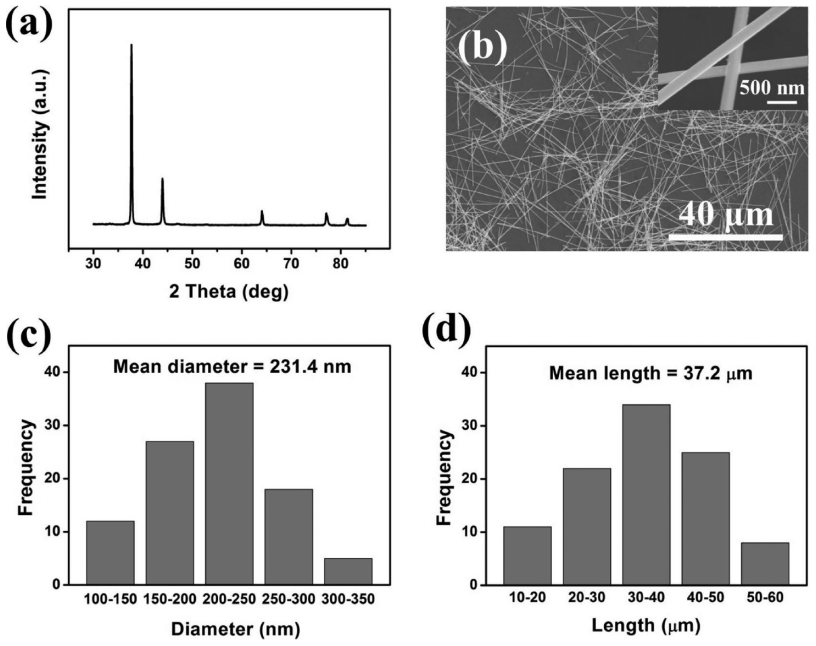


**Figure 1.** (a) XRD pattern, (b) SEM image, (c) diameter histogram, and (d) length histogram of Ag-NWs.

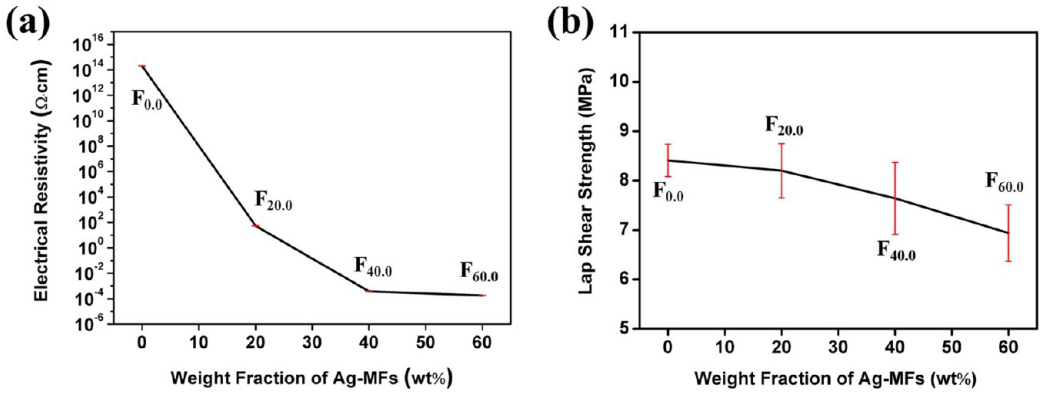


**Figure 2.** (a) Electrical resistivity (ER) and (b) LSS of the ECAs filled with single Ag-MFs.

ECAs was measured by a Keithley Source Meter 2400 device with a four-point probe, and the volume resistivity ($\rho$) can be calculated from the equation

$$\rho = R\frac{wt}{l} \tag{1}$$

where $R$ is the resistance of the sample and $l$, $w$, and $t$ are the length, width, and thickness of the sample, respectively.[8,10]

The samples for LSS test were prepared according to the recommendation of GB7124−1986. The adherends used were LY12-CZ aluminum alloy sheets with a dimension of 100 mm × 25 mm × 2 mm. They were polished with emery papers and the polished surfaces were greased with acetone and then dried. Afterward, two rectangular aluminum alloy sheets with an overlap length of 12.5 mm were fixed with the as-prepared epoxy adhesives. Then the samples were heated at 150 °C for 2 h. The schematic of preparing the sample is shown in Supporting Information Figure S2b as done in our previous work.[44] Measurement of the LSS of the ECAs was conducted by an electronic universal testing machine (Model RG-T-20A). The LSS ($\tau$) can be calculated from the equation

$$\tau = \frac{P}{BL} \tag{2}$$

where $B$ and $L$ are the length and width of the bonding part of the sample and $P$ is the force applied to break the bond.[8,10,44]

## RESULTS AND DISCUSSION

The broad peaks at $2\theta$ = 38.0°, 44.2°, 64.3°, 77.4°, and 81.4° are observed by the XRD pattern of the Ag-NWs as shown in Figure 1a, which correspond respectively to the (111), (200), (220), (311), and (222) reflection of Ag. These broad peaks match well with the data from the JCPDS file (no. 04-0783) for Ag. The SEM image of the as-prepared Ag-NWs is presented in Figure 1b, from which the length and diameter of Ag-NWs can be obtained. Figure 1c and d shows the length and diameter distributions of Ag-NWs, which are acquired from a series of SEM images as shown in Figure 1b using a computer software (Nano Measurer Software). The average length and diameter of Ag-NWs are measured to be 37.2 $\mu$m and 231.4 nm, respectively. And the average aspect ratio of Ag-NWs is estimated to be about 161.

As expected, both the electrical resistivity (ER) and the LSS of the ECAs filled with single Ag-MFs decrease with increasing the content of Ag-MFs as shown in Figure 2a and b. So, more Ag-MFs can lead to better conductive performance while worse adhesive strength. Compared to the $y$-axis scale, the error bars of Figure 2a are too small to be clearly seen and are then also given in Table 1. Moreover, it is observed that the conductive


DOI: 10.1021/acsami.5b00470
ACS Appl. Mater. Interfaces 2015, 7, 8041−8052

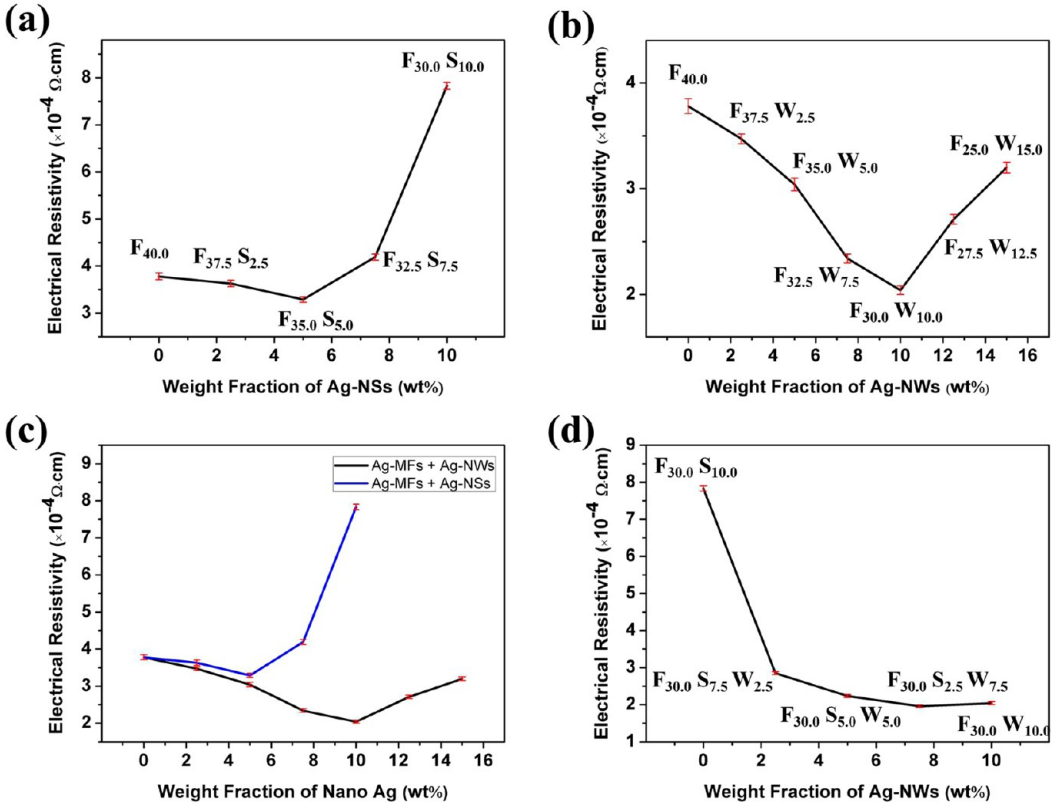


**Figure 3.** (a) ER of the binary hybrid ECAs filled with Ag-MFs and Ag-NSs, (b) ER of the binary hybrid ECAs filled with Ag-MFs and Ag-NWs, (c) comparison of the ER of two binary hybrid ECAs, and (d) ER of the ternary hybrid ECAs filled with Ag-MFs, Ag-NSs, and Ag-NWs.

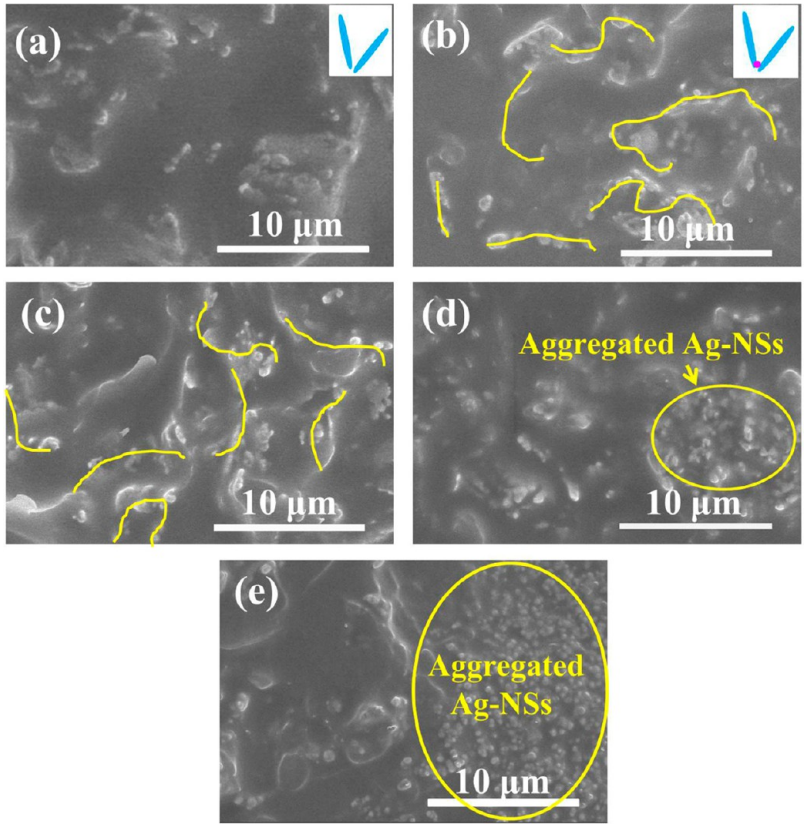


**Figure 4.** SEM images of the cross sections of (a) the single adhesive filled with 40 wt % Ag-MFs, the binary hybrid adhesives with (b) 37.5 wt % Ag-MFs and 2.5 wt % Ag-NSs, (c) 35 wt % Ag-MFs and 5 wt % Ag-NSs, (d) 32.5 wt % Ag-MFs and 7.5 wt % Ag-NSs, and (e) 30 wt % Ag-MFs and 10 wt % Ag-NSs.



DOI: 10.1021/acsami.5b00470
ACS Appl. Mater. Interfaces 2015, 7, 8041−8052

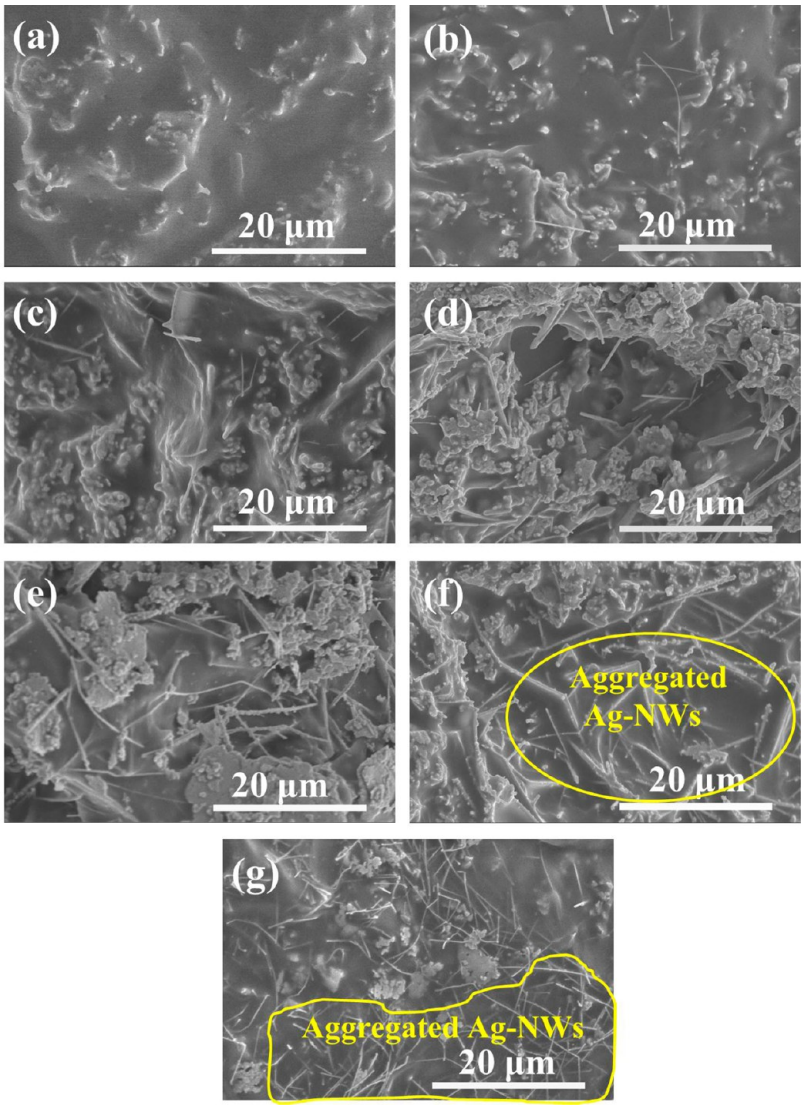


**Figure 5.** SEM images of the cross sections of (a) the single ECA filled with 40 wt % Ag-MFs, the binary hybrid adhesives with (b) 37.5 wt % Ag-MFs and 2.5 wt % Ag-NWs, (c) 35 wt % Ag-MFs and 5 wt % Ag-NWs, (d) 32.5 wt % Ag-MFs and 7.5 wt % Ag-NWs, (e) 30 wt % Ag-MFs and 10 wt % Ag-NWs, (f) 27.5 wt % Ag-MFs and 12.5 wt % Ag-NWs, and (g) 25 wt % Ag-MFs and 15 wt % Ag-NWs.

performance of the 40 wt % Ag-MF ECA is in the same order of magnitude with that of the 60 wt % Ag-MF ECA. On the other hand, the LSS of the 40 wt % Ag-MF ECA is higher than that of the 60 wt % Ag-MF ECA. Therefore, the total amount of Ag fillers in the ECAs will be set at 40 wt % for the purpose of achieving excellent overall performance.

The results for the electrical property of binary and ternary hybrid adhesives are presented in Figure 3a–d. As shown in Figure 3a, the electrical resistivity of the ECAs filled with Ag-MFs and Ag-NSs decreases initially with increasing the Ag NS content up to 5 wt % and then increases with further increasing the Ag NS content. The total resistance of an ECA is the sum of the bulk resistance ($R_b$) of fillers and the interface contact resistance ($R_i$) between neighboring fillers.[21,22] $R_i$ is made up of constriction resistance ($R_c$) and tunneling resistance ($R_t$). The constriction resistance comes from the spots where fillers are directly contacted. It increases with increasing the number of contact points, and decreases with increasing the contact area. The tunneling resistance comes from the spots where fillers are not directly contacted, and the electrons need to overcome barrier energy to transfer through those spots.[11,21,22,39] For the ECA filled with Ag-MFs only, there are many gaps between Ag-MFs as shown in Figure 4a. When a small amount of Ag-NSs is added, the Ag-NSs can be inserted between the gaps of Ag-MFs, so some Ag-MFs with small gaps can be connected by Ag-NSs as shown in the inset of Figure 4b. Hence, more electrically conductive channels are formed as indicated by yellow lines in Figure 4b and c, which will lead to a sharp decrease in the tunneling resistance.[39] On the other hand, the addition of Ag-NSs will lead to a slight increase in the constriction resistance.[39] But it cannot play a decisive role when the content of Ag-NSs is low. Therefore, from these two aspects, the interface contact resistance decreases and as a result, the ER of the ECAs decreases as the content of Ag-NSs increases. When the added Ag-NSs exceed a certain amount, the Ag-NSs at a high content will easily get aggregated as shown in Figure 4d and e, which will create adverse effects to the conductive paths.[45] The aggregated Ag-NSs cannot connect the Ag-MFs as the uniformly dispersed Ag-NSs, so the tunneling resistance could not be decreased a lot.[39] But the number of contact points between conductive Ag fillers will increase as the Ag-NS content increases, which will


DOI: 10.1021/acsami.5b00470
ACS Appl. Mater. Interfaces 2015, 7, 8041–8052

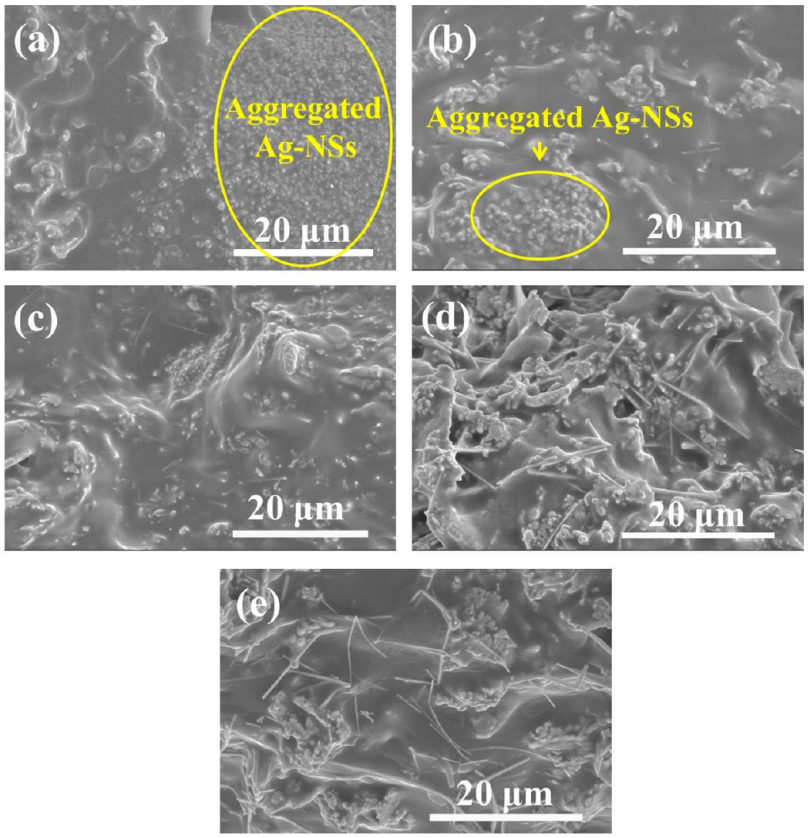


**Figure 6.** SEM images of the cross sections of (a) the binary hybrid adhesive filled with 30 wt % Ag-MFs and 10 wt % Ag-NSs, the ternary hybrid adhesives with (b) 30 wt % Ag-MFs, 7.5 wt % Ag-NSs, and 2.5 wt % Ag-NWs, (c) 30 wt % Ag-MFs, 5 wt % Ag-NSs, and 5 wt % Ag-NWs, (d) 30 wt % Ag-MFs, 2.5 wt % Ag-NSs, and 7.5 wt % Ag-NWs, and (e) the binary hybrid adhesive with 30 wt % Ag-MFs and 10 wt % Ag-NWs.

**Table 3. Comparison of the ΔEC[a] of the Binary and Ternary Hybrid ECAs**

| | Ag fillers | | | | |
|---|---|---|---|---|---|
| Sample code | Ag-MFs (wt %) | Ag-NSs (wt %) | Ag-NWs (wt %) | EC (S/cm) | ΔEC (S/cm) |
| $F_{37.5}$ $S_{2.5}$ | 37.5 | 2.5 | 0 | 2754 ± 54 | 109 |
| $F_{32.5}$ $W_{7.5}$ | 32.5 | 0 | 7.5 | 4273 ± 80 | 1628 |
| $F_{30.0}$ $S_{2.5}W_{7.5}$ | 30.0 | 2.5 | 7.5 | 5102 ± 92 | 2456 (>109 + 1628) |
| $F_{35.0}$ $S_{5.0}$ | 35.0 | 5.0 | 0 | 3040 ± 52 | 395 |
| $F_{35.0}$ $W_{5.0}$ | 35.0 | 0 | 5.0 | 3289 ± 65 | 644 |
| $F_{30.0}$ $S_{5.0}$ $W_{5.0}$ | 30.0 | 5.0 | 5.0 | 4484 ± 83 | 1839 (>395 + 644) |
| $F_{32.5}$ $S_{7.5}$ | 32.5 | 7.5 | 0 | 2387 ± 40 | −258 |
| $F_{37.5}$ $W_{2.5}$ | 37.5 | 0 | 2.5 | 2882 ± 38 | 237 |
| $F_{30.0}$ $S_{7.5}W_{2.5}$ | 30.0 | 7.5 | 2.5 | 3509 ± 49 | 864 (>−258+ 237) |

[a]Note: ΔEC = EC (binary or ternary hybrid) − EC (40 wt % single Ag-MFs).

lead to a sharp increase in the constriction resistance.[39,46] So, the interface contact resistance increases. Consequently, the ER of the ECAs increases as the Ag-NS content increases further over 5 wt %.

As shown in Figure 3b, the ER of the ECAs filled with Ag-MFs and Ag-NWs decreases initially with increasing the Ag-NW content until 10 wt % and then increases with further increasing the Ag-NW content. The average aspect ratio of the Ag-NWs is around 161, which is much higher than that (about 40) of Ag-MFs. When a small amount of Ag-NWs is added to the Ag-MFs, the Ag-NWs play a bridging role among the Ag-MFs that did not connect before. Thus, more electrically conductive channels are formed by Ag-NWs as shown in Figure 5b−e, leading to a sharp decrease in the tunneling resistance.[39] On the other hand, the constriction resistance is slightly increased because of the addition of a small amount of Ag-NWs. On the basis of the above two effects, the interface contact resistance decreases. As a result, the ER of the ECAs is decreased by the addition of a small amount of Ag-NWs. As the content of Ag-NWs increases further, the amount of Ag-MFs decreases. The original electrically conductive channels formed by Ag-MFs are destroyed when the Ag-NWs exceeds a certain amount. New electrically conductive channels are formed by a large amount of Ag-NWs and the rest of Ag-MFs as shown in Figure 5f and g. Moreover, the Ag-NWs at such a high content will also get aggregated, although not as badly as Ag-NSs, which will create adverse effects to the conductive paths.[45] The aggregated Ag-NWs cannot bridge the Ag-MFs as the dispersed Ag-NWs. Hence, the tunneling resistance cannot be decreased a lot.[39] On the other hand, the number of contact points is dramatically increased when the content of Ag-NWs is increased to a high level, and thus the constriction resistance is greatly increased.[39,46] So, the interface contact resistance increases. Finally, the ER of the ECAs increases as the Ag-NW content increases further over 10 wt %.

A comparison is made for the ER of the binary hybrid ECAs filled with Ag-MFs and Ag-NWs with that of the binary hybrid ECAs filled with Ag-MFs and Ag-NSs as a function of the conductive nanofiller content as shown in Figure 3c. On the one hand, it can be seen that the two trends are similar. The ER of the two series of the ECAs both decreases first to the lowest value as the content of the conductive nanofiller content


DOI: 10.1021/acsami.5b00470
ACS Appl. Mater. Interfaces 2015, 7, 8041−8052

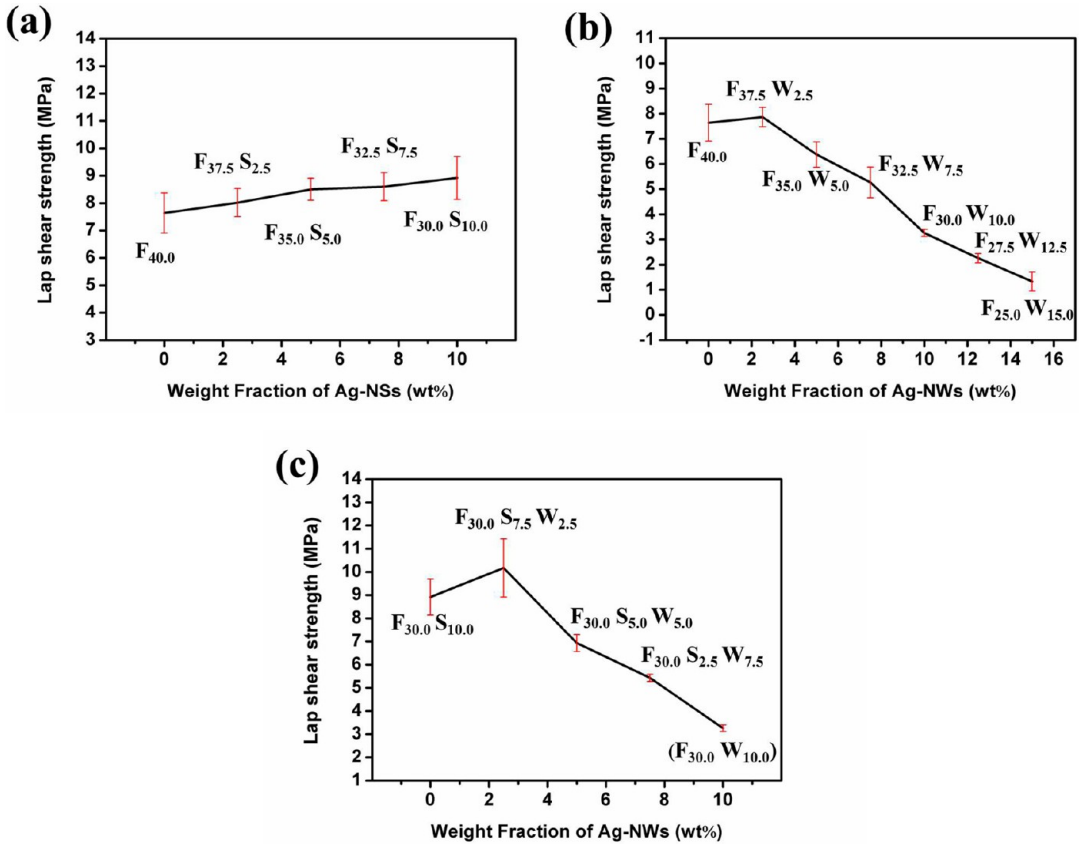


**Figure 7.** LSS of (a) the binary hybrid ECAs filled with Ag-MFs and Ag-NSs, (b) the binary hybrid ECAs filled with Ag-MFs and Ag-NWs, and (c) the ternary hybrid ECAs filled with Ag-MFs, Ag-NSs, and Ag-NWs.

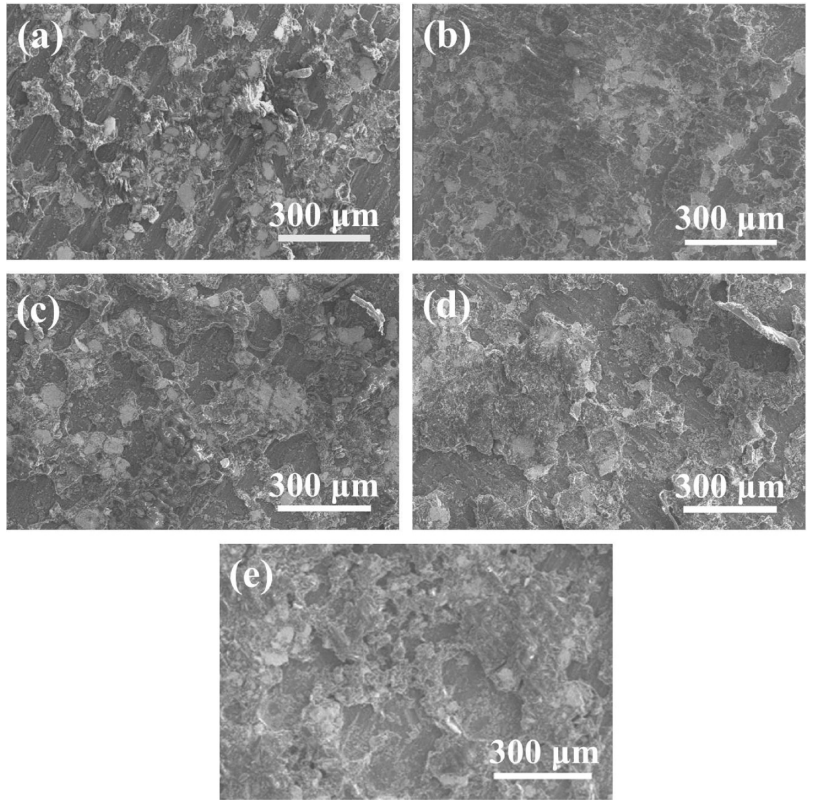


**Figure 8.** SEM images of the lap shear fracture surfaces of (a) the single adhesive filled with 40 wt % Ag-MFs, the binary hybrid adhesives with (b) 37.5 wt % Ag-MFs and 2.5 wt % Ag-NSs, (c) 35 wt % Ag-MFs and 5 wt % Ag-NSs, (d) 32.5 wt % Ag-MFs and 7.5 wt % Ag-NSs, and (e) 30 wt % Ag-MFs and 10 wt % Ag-NSs.



DOI: 10.1021/acsami.5b00470
*ACS Appl. Mater. Interfaces* 2015, 7, 8041−8052

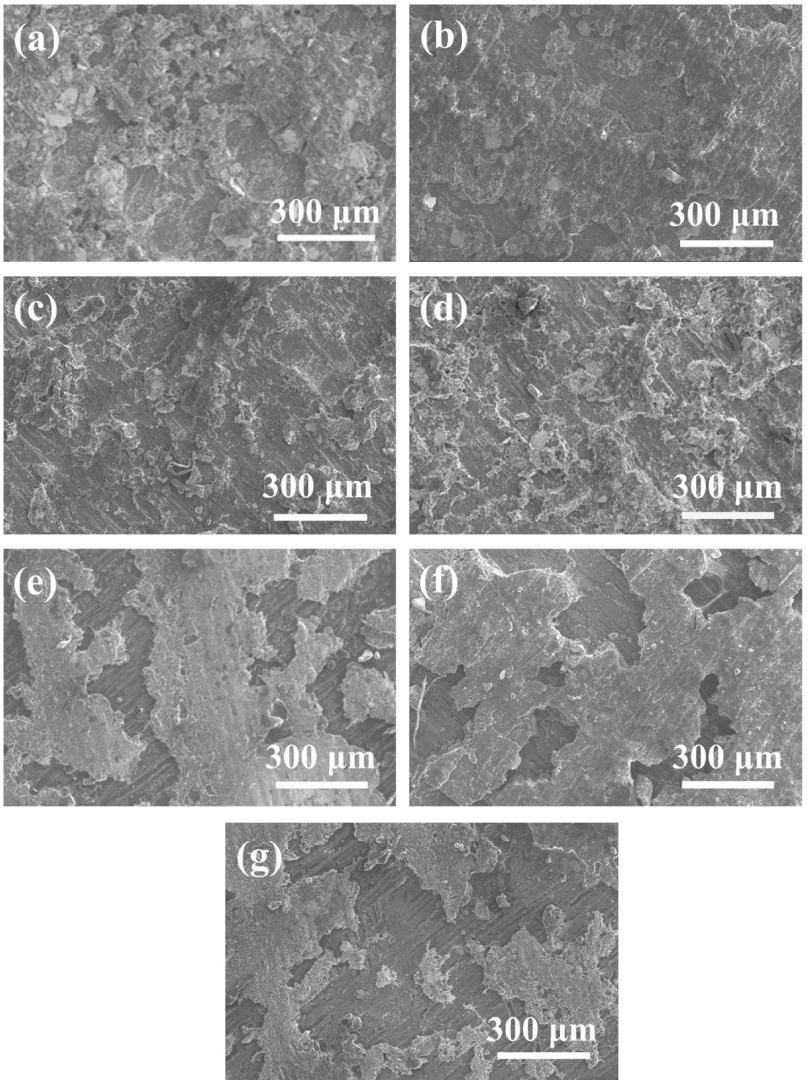


**Figure 9.** SEM images of the lap shear fracture surfaces of (a) the single adhesive filled with 40 wt % Ag-MFs, the binary hybrid adhesives with (b) 37.5 wt % Ag-MFs and 2.5 wt % Ag-NWs, (c) 35 wt % Ag-MFs and 5 wt % Ag-NWs, (d) 32.5 wt % Ag-MFs and 7.5 wt % Ag-NWs, (e) 30 wt % Ag-MFs and 10 wt % Ag-NWs, (f) 27.5 wt % Ag-MFs and 12.5 wt % Ag-NWs, and (g) 25 wt % Ag-MFs and 15 wt % Ag-NWs.

increases, and afterward increases as the content of the conductive nanofiller content increases further. Therefore, both the Ag-NSs and the Ag-NWs with appropriate filler contents can improve the EC of the ECAs filled with single Ag-MFs. On the other hand, the Ag-NWs can improve the EC of ECAs to a much larger degree than the Ag-NSs, indicating that the Ag-NWs with a large aspect ratio can more easily form conductive networks than the Ag-NSs.

As shown in Figure 3d, the ER of the ternary hybrid ECAs decreases as the content of Ag-NWs increases while the content of Ag-NSs decreases. First, the average aspect ratio (161) of the Ag-NWs is much higher than that (unity) of Ag-NSs, a high aspect ratio is beneficial for building the conductive network.[7,21−23] Second, when the Ag-NS content is higher than 5.0 wt %, the Ag-NSs can easily get aggregated as shown in Figure 6a and b, and the aggregated Ag-NSs will worsen the EC of the adhesives.[45] Additional Ag fillers are required to form an electrical conductive network due to the formation of Ag-NS aggregates.[45] Third, the number of contact points between Ag fillers will increase dramatically when the content of Ag-NSs increases while the content of Ag-NWs decreases, leading to a sharp increase of the constriction resistance.[39,46] As a result, the interface contact resistance increases and the EC of the ternary hybrid adhesives becomes relatively low.

On the other hand, when the amount of Ag-NSs is less than 5 wt % while the amount of Ag-NWs is more than 5 wt % as shown in Figure 6d and e, the Ag-NSs can be dispersed uniformly, and they can be inserted between the gaps of Ag-MFs. Meanwhile, the Ag-NWs play a bridging role among the Ag-MFs that did not connect before. As a result, more electrically conductive channels can be formed, leading to a sharp decrease of the tunneling resistance.[39] Finally, the EC of the ternary hybrid adhesives increases as the Ag-NW content increases while the Ag-NS content decreases.

Moreover, Ag-NSs and Ag-NWs with appropriate filler contents show novel synergistic effects in improving the EC of the ECAs. The synergistic effect is that the two factors produce an effect greater than the sum of their individual effects. Since the standard deviations relative to the average values are less than 2%, the improvement in the EC of the ECAs achieved by replacing partial Ag-MFs with 2.5 wt % Ag-NSs and 7.5 wt % Ag-NWs is obviously larger than the summed improvement in


DOI: 10.1021/acsami.5b00470
ACS Appl. Mater. Interfaces 2015, 7, 8041−8052

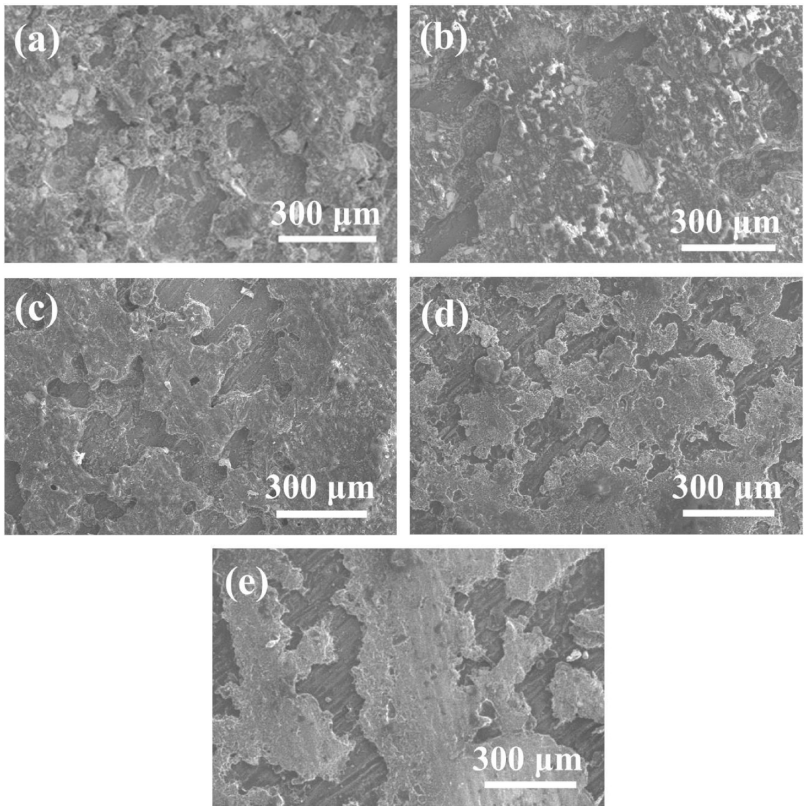


**Figure 10.** SEM images of the lap shear fracture surfaces of (a) the binary hybrid adhesive with 30 wt % Ag-MFs and 10 wt % Ag-NSs, the ternary hybrid adhesives with (b) 30 wt % Ag-MFs, 7.5 wt % Ag-NSs, and 2.5 wt % Ag-NWs, (c) 30 wt % Ag-MFs, 5 wt % Ag-NSs, and 5 wt % Ag-NWs, (d) 30 wt % Ag-MFs, 2.5 wt % Ag-NSs, and 7.5 wt % Ag-NWs, and (e) the binary hybrid adhesive with the 30 wt % Ag-MFs and 10 wt % Ag-NWs.

**Table 4. Comparison of the ER of the As-Prepared Ternary Hybrid ECA with That of the ECAs Reported Previously**

| filler | content (wt %) | ER (Ω cm) | refs |
|---|---|---|---|
| 1 Ag-MSs/1 Ag-NSs | 33 | 2.48 | 48 |
| 1 Ag-MSs/3Ag-NSs | 33 | $10^2$ | |
| 3 Ag-MSs/1 Ag-NSs | 33 | $10^4$ | |
| Ag-MSs | 40 | $10^2$ | 16 |
| Ag-MFs | 40 | $10^1$ | |
| Ag-MSs | 56 | 3.64 | 21 |
| Ag-NSs | 56 | $3.65 \times 10^{-1}$ | |
| Ag-NWs | 56 | $1.2 \times 10^{-4}$ | |
| Ag-MSs | 75 | $7.5 \times 10^{-4}$ | |
| Ag-MFs | 50 | $9.3 \times 10^{-4}$ | 38 |
| Ag-MFs | 60 | $5.1 \times 10^{-4}$ | |
| 5 Ag-MFs/1 Ag nanodendrites | 60 | $1.3 \times 10^{-4}$ | |
| Ag-NWs | 53 | $1.9 \times 10^{-4}$ | 7 |
| Ag-MSs | 73 | $5.3 \times 10^{-4}$ | |
| Ag-NSs | 75 | $1.4 \times 10^{-3}$ | |
| Ag-MFs | 70 | $4.23 \times 10^{-3}$ | 11 |
| Ag-MSs | 70 | $7.21 \times 10^{-3}$ | |
| 1 Ag-MSs/1 Ag-NSs | 70 | 5.88 | |
| 4 Ag-MSs/1 Ag-NSs | 70 | 0.36 | |
| Ag-NSs | 70 | nonconductive | |
| Ag-MFs | 75 | $2.4 \times 10^{-4}$ | 13 |
| Ag-MFs | 76 | $4.77 \times 10^{-4}$ | 12 |
| ternary hybrid Ag fillers ($F_{30.0}$ $S_{7.5}$ $W_{2.5}$) | 40 | $2.85 \times 10^{-4}$ | present work |

the EC of the ECAs achieved by replacing the Ag-MFs with 2.5 wt % Ag-NSs and 7.5 wt % Ag-NWs independently as shown in Table 3. Therefore, it can be concluded that the simultaneous introduction of Ag-NSs and Ag-NWs can lead to a positive synergistic effect in enhancing the EC of the conductive epoxy adhesives. In addition, for the binary hybrid adhesive with 30 wt % Ag-MFs and 10 wt % Ag-NWs, the Ag-NWs are uniformly dispersed in the adhesive and thus the corresponding EC is high as shown in Figure 3. Nonetheless, the adhesive property for this binary hybrid adhesive is quite poor due to a high Ag-NW content to be shown later in this work. So, this is not the adhesive with a high overall performance we want.

Adhesive joints may fail adhesively or cohesively. In adhesive failure, the separation occurs between the adhesive layer and one of the adherends. In cohesive failure, the separation occurs in such a manner that both adherend surfaces remain covered with the adhesive. Cohesive failure is the ideal type of failure because for this failure the maximum strength of the materials in the joint can be reached.[47] The results for the LSS of the binary hybrid ECAs and the ternary hybrid ECAs are presented in Figure 7. SEM images are given in Figures 8−10 for the adherend surfaces after the failure of the adhesives.

As shown in Figure 7a, the LSS of the binary hybrid ECAs filled with Ag-MFs and Ag-NSs increases slightly as the content of Ag-NSs increases. The adherend surfaces are almost fully covered by the binary hybrid adhesives and the amount of the ECAs covered on the adherend surfaces is large as shown in Figure 8. So, all the adhesives fail in a cohesive manner. Moreover, it seems from Figure 8 that the amount of the adhesives


DOI: 10.1021/acsami.5b00470
ACS Appl. Mater. Interfaces 2015, 7, 8041−8052

Table 5. Comparison of the As-Prepared Ternary Hybrid ECA with Commercial ECAs

| company | model | filler (wt %) | ER (Ω cm) | LSS (MPa) |
|---|---|---|---|---|
| Epoxy Technology, USA | ED1021 | 70−80 | $2 \times 10^{-4}$ | |
| | E20S-D | 60−75 | $1.4 \times 10^{-4}$ | |
| Sumitomo, Japan Henkel, Germany | T-3007−20 | 78−82 | $4.9 \times 10^{-4}$ | |
| | ABLEBOND 8290 | 60−100 | $8 \times 10^{-3}$ | |
| | ABLESTIK C 850−5A | 60−100 | $1 \times 10^{-3}$ | |
| | ABLEBOND 84−1LMI | 60−100 | $5 \times 10^{-4}$ | |
| | ABLEBONDAAA3131A | 60−100 | $5 \times 10^{-5}$ | |
| | ABLEBOND84−1LMISR4 | 60−100 | $2 \times 10^{-4}$ | 8.55 ± 0.34 |
| Shenzhen Capiton Sci-Technology, China | CAPITON-924 K | 65 | $3 \times 10^{-4}$ | 2.62 ± 0.44 |
| present work | Ternary hybrid ECA ($F_{30.0}$ $S_{7.5}$ $W_{2.5}$) | 40 | $2.85 \times 10^{-4}$ | 10.17 ± 1.25 |

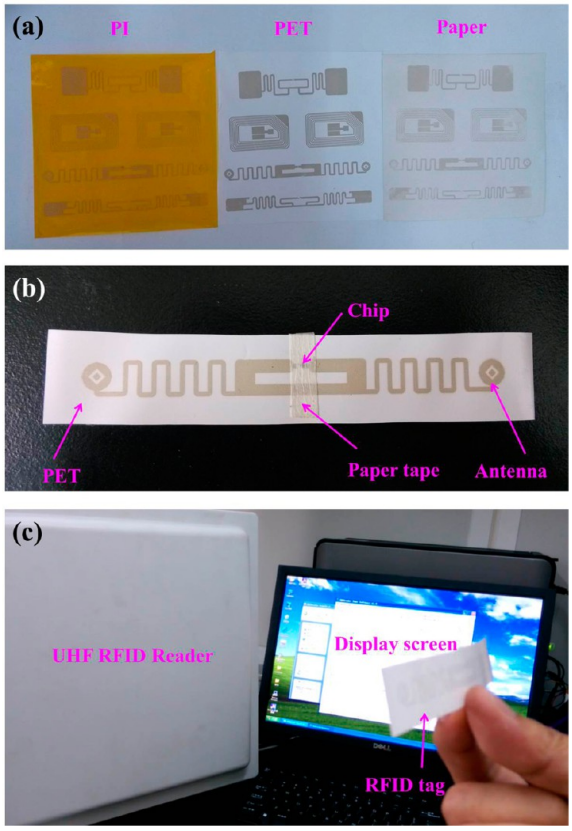


**Figure 11.** Photographs of (a) the RFID antennas printed on various substrate materials using the ternary hybrid ECA with the optimal formulation, (b) the complete RFID tag based on PET substrate, and (c) showing of the reading of the as-prepared RFID tag.

covered on the adherend surfaces increases slightly as the Ag-NS content increases. This is possibly because the specific surface area of the Ag-NSs is larger than that of Ag-MFs and thus it is relatively easier for the epoxy resin to wet Ag-NSs compared to Ag-MFs.[21,38] This is consistent with the observation that the LSS of the binary hybrid adhesives increases slightly as the content of Ag-NSs increases as shown in Figure 7a.

As shown in Figure 7b, the LSS of the binary hybrid ECAs filled with Ag-MFs and Ag-NWs is enhanced only when Ag-NWs have a low content of 2.5 wt %. But the LSS of the binary hybrid adhesives decreases as the content of Ag-NWs increases further. It can be seen from Figure 9a and b that the amount of the ECAs covered on the adherend surfaces is large at a low Ag-NW content. The adhesives with a low Ag-NW content fail in a cohesive manner and thus the LSS is high. However, the amount of ECAs on the adherend surfaces decreases and the uncovered adherend surface area becomes larger as the Ag-NW content increases. It is thus clear that the binary hybrid adhesives show a failure trend from cohesive to adhesive ones as the Ag-NW content increases. As a result, the LSS of the adhesives is low at a high Ag-NW content.

As shown in Figure 7c, the LSS of the ternary hybrid ECAs filled with Ag-MFs, Ag-NSs and Ag-NWs increases first as the content of Ag-NWs increases up to 2.5 wt %, and afterward decreases dramatically as the content of Ag-NWs increases further. When the content of Ag-NSs is more than 5 wt % and the amount of Ag-NWs is less than 5 wt % as shown in Figure 10a and b, the amount of ECAs covered on the adherend surfaces is large. Hence, these samples fail cohesively and the LSS is high. However, when the amount of Ag-NWs is more than 5 wt %as shown in Figure 10d and e, the amount of ECAs covered on the adherend surfaces decreases as the Ag-NW content increases. Therefore, these samples trend toward adhesive failure. It is thus understandable that these samples have a relatively low LSS.

Taking into consideration both the EC performance and the adhesive strength, the optimal ternary hybrid ECA is obtained at the contents of 30.0 wt % Ag-MFs, 7.5 wt % Ag-NSs, and 2.5 wt % Ag-NWs. A comparison is made between the ER of the as-prepared ternary hybrid ECA and that of the ECAs reported previously in the literature.[7,11−13,16,21,38,48] As shown in Table 4, the ER of the ternary hybrid ECA is much lower than that of most of the ECAs reported previously with similar Ag contents or even more than 70 wt % Ag fillers.

The ER of the optimal ternary hybrid ECA is $2.85 \times 10^{-4}$ Ω cm, which is in the ER range of $10^{-3}$−$10^{-5}$ Ω cm for commercial conductive adhesives with a much higher Ag content of 60−100 wt % as shown in Table 5. Also, the LSS of the as-prepared ternary hybrid ECA is compared with that of two commercial ECAs using the same test method under the same testing condition. As shown in Table 5, the LSS of the as-prepared ternary hybrid ECA is higher than that of the two commercial ECAs, which is most likely due to the fact that the low content of Ag fillers is used in the present work. Therefore, the ternary hybrid adhesive prepared in the present study is superior to the commercial adhesives in terms of its overall performance and cost.

Radio frequency identification (RFID) technology uses radio waves to identify objects without making any physical contact. RFID technology has become part of our daily lives and can be found in car keys, employee identification, medical history/billing, highway toll tags and security access cards.[49] For ECAs, one of the immediate applications is to use them for printing


DOI: 10.1021/acsami.5b00470
ACS Appl. Mater. Interfaces 2015, 7, 8041−8052

the RFID tag antennas. In this work, the ternary hybrid ECA due to its good adhesive property can be well printed on various substrates such as polyethylene terephthalate (PET), polyimide (PI), and paper, as shown in Figure 11a. The complete RFID tag after fixing a chip based on PET substrate is prepared as shown in Figure 11b. As a comparison, a RFID tag with the commercial ECA (CAPITON-924 K, 65 wt % Ag-MFs) is also prepared. The reading distances of both the RFID tags are about 2.5 m. Since the amount (40 wt %) of Ag in the present study is much less than that of the commercial ECA (65 wt % Ag), the low silver content in the as-prepared ternary ECA will lead to an excellent LSS as shown above and meanwhile its cost is much lower. Therefore, the ternary hybrid ECA is definitely superior to the commercial ECA in various practical applications including RFID antenna production etc.

## CONCLUSIONS

In summary, the ternary hybrid silver/epoxy adhesive with an excellent overall performance has been prepared by introducing appropriate contents of Ag-MFs, Ag-NSs, and Ag-NWs into an epoxy matrix. A small amount of Ag-NSs or Ag-NWs can dramatically improve the EC of the ECAs filled with single Ag-MFs. The Ag-NSs and Ag-NWs with appropriate contents have a synergistic effect in improving the EC of the ECAs. The as-prepared ternary hybrid ECA with the 40 wt % Ag shows an excellent EC which is much higher than that of the traditional ECAs filled with equal amounts of single Ag-MFs. Meanwhile, the LSS of the ternary hybrid ECA is better than the commercial ECAs with a much higher Ag content. Therefore, the as-prepared low silver content ternary hybrid ECA with an excellent overall performance is obviously superior to the commercial ECAs or those reported previously normally with a much higher silver content. Finally, RFID tag antennas have been successfully printed with the ternary hybrid ECA as an immediate application example.

## ASSOCIATED CONTENT

### Supporting Information

Particle size distributions of Ag-MFs and Ag-NSs, SEM images of Ag-MFs and Ag-NSs, schematics of the samples for electrical performance test and mechanical property test, and the process of reading of the as-prepared RFID tag. This material is available free of charge via the Internet at http://pubs.acs.org.

## AUTHOR INFORMATION

### Corresponding Author

*Tel./Fax.: +86-10-8254-3752. E-mail: syfu@mail.ipc.ac.cn.

### Author Contributions

The manuscript was written through contributions of all authors. All authors have given approval to the final version of the manuscript.

### Notes

The authors declare no competing financial interest.

## ACKNOWLEDGMENTS

This work is supported by National Natural Science Foundation of China (No. 11002142, 51373187, and 11372312).

## REFERENCES

(1) Li, Y.; Moon, K. S.; Wong, C. P. Electronics Without Lead. *Science* **2005**, *308*, 1419−1420.

(2) Li, Y.; Wong, C. P. Recent Advances of Conductive Adhesives as a Lead-Free Alternative in Electronic Packaging: Materials, Processing, Reliability and Applications. *Mater. Sci. Eng., R* **2006**, *51*, 1−35.

(3) Mir, I.; Kumar, D. Recent Advances in Isotropic Conductive Adhesives for Electronics Packaging Applications. *Int. J. Adhes. Adhes.* **2008**, *28*, 362−371.

(4) Hsu, S. L. C.; Wu, R. T. Synthesis of Contamination-Free Silver Nanoparticle Suspensions for Micro-Interconnects. *Mater. Lett.* **2007**, *61*, 3719−3722.

(5) Lu, D. D.; Wong, C. P. Recent Advances in Developing High Performance Isotropic Conductive Adhesives. *J. Adhes. Sci. Technol.* **2008**, *22*, 835−851.

(6) Untereker, D.; Lyu, S.; Schley, J.; Martinez, G.; Lohstreter, L. Maximum Conductivity of Packed Nanoparticles and Their Polymer Composites. *ACS Appl. Mater. Interfaces* **2009**, *1*, 97−101.

(7) Tao, Y.; Xia, Y. P.; Wang, H.; Gong, F. H.; Wu, H. P.; Tao, G. L. Novel Isotropical Conductive Adhesives for Electronic Packaging Application. *IEEE Trans. Adv. Packag.* **2009**, *32*, 589−592.

(8) Tan, F. T.; Qiao, X. L.; Chen, J. G.; Wang, H. S. Effects of Coupling Agents on the Properties of Epoxy-Based Electrically Conductive Adhesives. *Int. J. Adhes. Adhes.* **2006**, *26*, 406−413.

(9) Zhang, Y.; Qi, S. H.; Wu, X. M.; Duan, G. C. Electrically Conductive Adhesive Based on Acrylate Resin Filled with Silver Plating Graphite Nanosheet. *Synth. Met.* **2011**, *161*, 516−522.

(10) Wu, H. P.; Wu, X. J.; Ge, M. Y.; Zhang, G. Q.; Wang, Y. W.; Jiang, J. Z. Effect Analysis of Filler Sizes on Percolation Threshold of Isotropical Conductive Adhesives. *Compos. Sci. Technol.* **2007**, *67*, 1116−1120.

(11) Ye, L. L.; Lai, Z. H.; Liu, J. H.; Tholen, A. Effect of Ag Particle Size on Electrical Conductivity of Isotropically Conductive Adhesives. *IEEE Trans. Electron. Packag. Manuf.* **1999**, *22*, 299−302.

(12) Cui, H. W.; Du, W. H. Novel Fast-Curing Electrically Conductive Adhesives from a Functional Epoxy and Micro Silver Flakes: Preparation, Characterization, and Humid-Thermal Aging. *J. Adhes.* **2013**, *89*, 714−726.

(13) Cui, H. W.; Fan, Q.; Li, D. S. Surface Functionalization of Micro Silver Flakes and Their Application in Electrically Conductive Adhesives for Electronic Package. *Int. J. Adhes. Adhes.* **2014**, *48*, 177−182.

(14) Yang, C.; Lin, W.; Li, Z. Y.; Zhang, R. W.; Wen, H. R.; Gao, B.; Chen, G. H.; Gao, P.; Yuen, M. M. F.; Wong, C. P. Water-Based Isotropically Conductive Adhesives: Towards Green and Low-Cost Flexible Electronics. *Adv. Funct. Mater.* **2011**, *21*, 4582−4588.

(15) Araki, T.; Sugahara, T.; Nogi, M.; Suganuma, K. Effect of Void Volume and Silver Loading on Strain Response of Electrical Resistance in Silver Flakes/Polyurethane Composite for Stretchable Conductors. *Jpn. J. Appl. Phys.* **2012**, *51*, No. 11PD01.

(16) Suriati, G.; Mariatti, M.; Azizan, A. Effects of Filler Shape and Size on the Properties of Silver Filled Epoxy Composite for Electronic Applications. *J. Mater. Sci.: Mater. Electron.* **2011**, *22*, 56−63.

(17) Song, L. N.; Myers, A. C.; Adams, J. J.; Zhu, Y. Stretchable and Reversibly Deformable Radio Frequency Antennas Based on Silver Nanowires. *ACS Appl. Mater. Interfaces* **2014**, *6*, 4248−4253.

(18) Miller, M. S.; O'Kane, J. C.; Niec, A.; Carmichael, R. S.; Carmichael, T. B. Silver Nanowire/Optical Adhesive Coatings as Transparent Electrodes for Flexible Electronics. *ACS Appl. Mater. Interfaces* **2013**, *5*, 10165−10172.

(19) Cao, X.; Liu, S. W.; Feng, Q. C.; Wang, N. Silver Nanowire-Based Electrochemical Immunoassay for Sensing Immunoglobulin G with Signal Amplification Using Strawberry-Like Zno Nanostructures as Labels. *Biosens. Bioelectron.* **2013**, *49*, 256−262.

(20) Yao, S. S.; Zhu, Y. Wearable Multifunctional Sensors Using Printed Stretchable Conductors Made of Silver Nanowires. *Nanoscale* **2014**, *6*, 2345−2352.

(21) Wu, H. P.; Liu, J. F.; Wu, X. J.; Ge, M. Y.; Wang, Y. W.; Zhang, G. Q.; Jiang, J. Z. High Conductivity of Isotropic Conductive Adhesives Filled with Silver Nanowires. *Int. J. Adhes. Adhes.* **2006**, *26*, 617−621.



DOI: 10.1021/acsami.5b00470
*ACS Appl. Mater. Interfaces* 2015, 7, 8041−8052

(22) Wu, H. P.; Wu, X. J.; Liu, J. F.; Zhang, G. Q.; Wang, Y. W.; Zeng, Y. W.; Jing, J. Z. Development of a Novel Isotropic Conductive Adhesive Filled with Silver Nanowires. *J. Compos. Mater.* **2006**, *40*, 1961−1969.
(23) Tao, Y.; Yang, Z. G.; Lu, X. L.; Tao, G. L.; Xia, Y. P.; Wu, H. P. Influence of Filler Morphology on Percolation Threshold of Isotropical Conductive Adhesives (ICA). *Sci. China: Technol. Sci.* **2012**, *55*, 28−33.
(24) Wu, H. P.; Wu, X. J.; Ge, M. Y.; Zhang, G. Q.; Wang, Y. W.; Jiang, J. Z. Properties Investigation on Isotropical Conductive Adhesives Filled with Silver Coated Carbon Nanotubes. *Compos. Sci. Technol.* **2007**, *67*, 1182−1186.
(25) Nguyen, H. V.; Andreassen, E.; Kristiansen, H.; Johannessen, R.; Hoivik, N.; Aasmundtveit, K. E. Rheological Characterization of a Novel Isotropic Conductive Adhesive-Epoxy Filled with Metal-Coated Polymer Spheres. *Mater. Des.* **2013**, *46*, 784−193.
(26) Nguyen, H. V.; Andreassen, E.; Kristiansen, H.; Aasmundtveit, K. E. Die Shear Testing of a Novel Isotropic Conductive Adhesive-Epoxy Filled With Metal-Coated Polymer Spheres. *IEEE Trans. Compon., Packag., Manuf. Technol.* **2013**, *3*, 1084−1093.
(27) Novák, I.; Krupa, I.; Chodák, I. Electroconductive Adhesives Based on Epoxy and Polyurethane Resins Filled with Silver-Coated Inorganic Fillers. *Synth. Met.* **2004**, *144*, 13−19.
(28) Nishikawa, H.; Mikami, S.; Miyake, K.; Aoki, A.; Takemoto, T. Effects of Silver Coating Covered with Copper Filler on Electrical Resistivity of Electrically Conductive Adhesives. *Mater. Trans.* **2010**, *51*, 1785−1789.
(29) Zhang, R. W.; Lin, W.; Lawrence, K.; Wong, C. P. Highly Reliable, Lowcost, Isotropically Conductive Adhesives Filled with Ag-Coated Cu Flakes for Electronic Packaging Applications. *Int. J. Adhes. Adhes.* **2010**, *30*, 403−407.
(30) Zhang, R. W.; Lin, W.; Moon, K. S.; Wong, C. P. Fast Preparation of Printable Highly Conductive Polymer Nanocomposites by Thermal Decomposition of Silver Carboxylate and Sintering of Silver Nanoparticles. *ACS Appl. Mater. Interfaces* **2010**, *2*, 2637−2645.
(31) Durairaj, R.; Man, L. W. Effect of epoxy and filler concentrations on curing behaviour of isotropic conductive adhesives. *J. Therm. Anal. Calorim.* **2011**, *105*, 151−155.
(32) Gao, H.; Liu, L.; Liu, K. H.; Luo, Y. F.; Jia, D. M.; Lu, J. S. Preparation of Highly Conductive Adhesives by in Situ Generated and Sintered Silver Nanoparticles During Curing Process. *J. Mater. Sci.: Mater. Electron.* **2012**, *23*, 22−30.
(33) Qiao, W. Y.; Bao, H.; Li, X. H.; Jin, S. L.; Gu, Z. M. Research on Electrical Conductive Adhesives Filled with Mixed Filler. *Int. J. Adhes. Adhes.* **2014**, *48*, 159−163.
(34) Jiang, H. J.; Moon, K. S.; Li, Y.; Wong, C. P. Surface Functionalized Silver Nanoparticles for Ultrahigh Conductive Polymer Composites. *Chem. Mater.* **2006**, *18*, 2969−2973.
(35) Cui, H. W.; Fan, Q.; Li, D. S. Novel Flexible Electrically Conductive Adhesives From Functional Epoxy, Flexibilizers, Micro-Silver Flakes and Nano-Silver Spheres for Electronic Packaging. *Polym. Int.* **2013**, *62*, 1644−1651.
(36) Chen, S. L.; Liu, K. H.; Luo, Y. F.; Jia, D. M.; Gao, H.; Hu, G. J.; Liu, L. In Situ Preparation and Sintering of Silver Nanoparticles for Low-Cost and Highly Reliable Conductive Adhesive. *Int. J. Adhes. Adhes.* **2013**, *45*, 138−143.
(37) Lee, H. H.; Chou, K. S.; Shih, Z. W. Effect of Nano-Sized Silver Particles on the Resistivity of Polymeric Conductive Adhesives. *Int. J. Adhes. Adhes.* **2005**, *25*, 437−441.
(38) Dai, K.; Zhu, G. P.; Lu, L. H.; Dawson, G. Easy and Large Scale Synthesis Silver Nanodendrites: Highly Effective Filler for Isotropic Conductive Adhesives. *J. Mater. Eng. Perform.* **2012**, *21*, 353−357.
(39) Amoli, B. M.; Marzbanrad, E.; Hu, A. M.; Zhou, Y. N.; Zhao, B. X. Electrical Conductive Adhesives Enhanced with High-Aspect-Ratio Silver Nanobelts. *Macromol. Mater. Eng.* **2014**, *299*, 739−747.
(40) Lu, D. Q.; Tong, Q. K.; Wong, C. P. Conductivity Mechanisms of Isotropic Conductive Adhesives (ICAs). *IEEE Trans. Electron. Packag. Manuf.* **1999**, *22*, 223−227.
(41) Chen, D. P.; Qiao, X. L.; Qiu, X. L.; Chen, J. G.; Jiang, R. Z. Large-Scale Synthesis of Silver Nanowires via a Solvothermal Method. *J. Mater. Sci.: Mater. Electron.* **2011**, *22*, 6−13.
(42) Li, N.; Huang, G. W.; Shen, X. J.; Xiao, H. M.; Fu, S. Y. Controllable Fabrication and Magnetic-Field Assisted Alignment of $Fe_3O_4$-Coated Ag Nanowires via a Facile Co-Precipitation Method. *J. Mater. Chem. C* **2013**, *1*, 4879−4884.
(43) Huang, G. W.; Xiao, H. M.; Fu, S. Y. Paper-Based Silver-Nanowire Electronic Circuits with Outstanding Electrical Conductivity and Extreme Bending Stability. *Nanoscale* **2014**, *6*, 8495−8502.
(44) Liu, Y.; Yang, G.; Xiao, H. M.; Feng, Q. P.; Fu, S. Y. Mechanical Properties of Cryogenic Epoxy Adhesives: Effects of Mixed Curing Agent Content. *Int. J. Adhes. Adhes.* **2013**, *41*, 113−118.
(45) Cho, H. W.; Nam, S. W.; Lim, S.; Kim, D.; Kim, H.; Sung, B. J. Effects of Size and Interparticle Interaction of Silica Nanoparticles on Dispersion and Electrical Conductivity of Silver/Epoxy Nanocomposites. *J. Appl. Phys.* **2014**, *115*, 154307.
(46) Taherian, R.; Hadianfard, M. J.; Golikand, A. N. A New Equation for Predicting Electrical Conductivity of Carbon-Filled Polymer Composites Used for Bipolar Plates of Fuel Cells. *J. Appl. Polym. Sci.* **2013**, *128*, 1497−1509.
(47) Ebnesajjad, S., Ed. *Adhesives Technology Handbook*, 2nd ed; William Andrew Publishing: Norwich, NY, 2008.
(48) Zulkarnain, M.; Mariatti, M.; Azid, I. A. Effects of Hybrid Fillers Based on Micro- and Nano-Sized Silver Particles on the Electrical Performance of Epoxy Composites. *J. Mater. Sci.: Mater. Electron.* **2013**, *24*, 1523−1529.
(49) Sangoi, R.; Smith, C. G.; Seymour, M. D.; Venkataraman, J. N.; Clark, D. M.; Kleper, M. L.; Kahn, B. E. Printing Radio Frequency Identification (RFID) Tag Antennas Using Inks Containing Silver Dispersions. *J. Dispersion. Sci. Technol.* **2004**, *25*, 513−521.


DOI: 10.1021/acsami.5b00470
*ACS Appl. Mater. Interfaces* 2015, 7, 8041−8052